BIOENGINEERING

Enhanced PEDOT adhesion on solid substrates with electrografted P(EDOT-NH_2)

Liangqi Ouyang,[1]* Bin Wei,[1] Chin-chen Kuo,[1] Sheevangi Pathak,[2] Brendan Farrell,[3] David C. Martin[1,3†]

Conjugated polymers, such as poly(3,4-ethylene dioxythiophene) (PEDOT), have emerged as promising materials for interfacing biomedical devices with tissue because of their relatively soft mechanical properties, versatile organic chemistry, and inherent ability to conduct both ions and electrons. However, their limited adhesion to substrates is a concern for in vivo applications. We report an electrografting method to create covalently bonded PEDOT on solid substrates. An amine-functionalized EDOT derivative (2,3-dihydrothieno[3,4-b][1,4]dioxin-2-yl)methanamine (EDOT-NH_2), was synthesized and then electrografted onto conducting substrates including platinum, iridium, and indium tin oxide. The electrografting process was performed under slightly basic conditions with an overpotential of ~2 to 3 V. A nonconjugated, cross-linked, and well-adherent P(EDOT-NH_2)–based polymer coating was obtained. We found that the P(EDOT-NH_2) polymer coating did not block the charge transport through the interface. Subsequent PEDOT electrochemical deposition onto P(EDOT-NH_2)–modified electrodes showed comparable electroactivity to pristine PEDOT coating. With P(EDOT-NH_2) as an anchoring layer, PEDOT coating showed greatly enhanced adhesion. The modified coating could withstand extensive ultrasonication (1 hour) without significant cracking or delamination, whereas PEDOT typically delaminated after seconds of sonication. Therefore, this is an effective means to selectively modify microelectrodes with highly adherent and highly conductive polymer coatings as direct neural interfaces.

INTRODUCTION

Poly(3,4-ethylene dioxythiophene) (PEDOT) is one of the most chemically stable conjugated polymers and can show high conductivities (more than 3000 S/cm in certain cases) (*1*, *2*). PEDOT has been widely used in applications such as energy conversion and storage, organic light-emitting diodes, electrochemical transistors, and sensing (*3*). In recent years, PEDOT has been used as the direct interfacing material between neural tissue and a variety of electronic biomedical devices (*4*–*9*). When electrochemically deposited onto solid microelectrodes (typically made of gold, iridium, and platinum), PEDOT turns the metallic surface into a soft, conformal, and high–surface area organic interface that supports both electron and ion transport (*10*). With PEDOT coatings on the electrodes, the performance of biomedical devices, both in vivo and in vitro, is significantly improved (*11*–*13*). The versatile organic chemistry of these coatings also allows for construction of nanostructures with templates (*14*) and codeposition or modification with biologically active substances such as anti-inflammatory drugs or cell growth factors to modulate tissue responses after implantation (*13*, *15*–*18*).

However, in some cases, the low mechanical stability and relatively limited adhesion of conjugated polymers on solid substrates can limit the lifetime and performance of the devices (*19*–*24*). Upon mechanical deformation (*25*), sterilization (*26*), or prolonged charge injection (*23*), PEDOT can crack and delaminate from the substrate, significantly affecting the device performance. Electrochemically deposited PEDOT on neural probes has shown signs of similar mechanical failures after chronic implantations in vivo (*27*, *28*). For implantable devices, the mechanical failures may lead to the loss of electroactivity and might also leave behind undesirable residue in the tissue. Although the film stiffness and strength can be improved through cross-linking (*29*), an important limitation is that, in the typical methods of preparation, there are no specific chemical interactions expected between the conjugated polymer and the inorganic substrate. The electrochemical deposition of solid conjugated polymers from precursor solutions of monomer onto various substrates is mainly driven by their limited solubility as the molecular weight increases. When the solubility of the conjugated polymer in the reaction solvent is increased, less satisfactory deposition or even no deposition is usually observed (*30*, *31*). Furthermore, when the conjugated polymer films become thicker, they tend to be less adhesive to the underlying surface (*19*).

Several previous approaches intended to increase interfacial interactions have been shown to significantly improve the adhesion of conjugated polymers on solids. For example, roughened substrate surfaces provide mechanical interlocking for the better attachment of deposited materials (*32*). The adhesion and cycling stability of conducting polymer coatings can therefore be improved on fuzzy gold or laser-roughened platinum surfaces (*26*, *33*). The relative surface energy of the substrate and the polymers themselves is also expected to play a role in polymer adhesion. For example, relatively hydrophilic conducting polymers, such as polypyrrole and polyaniline, would strongly adhere to hydrophilic substrates (*34*–*36*). Changing the surface chemistry of the substrate can tune the adhesion of conducting polymers. One such approach involves using bifunctional molecules to form self-assembled monolayers (SAMs) on the substrate through the well-known specific interactions between thiols and gold or platinum (*37*, *38*). An SAM of monomer-functionalized thiols coated onto gold or platinum substrates resulted in improved adhesion of subsequently deposited conducting polymers (*39*, *40*). Covalent bonding on substrates can also be achieved using monomer-functionalized silanes to form chemical bonds with metals or indium tin oxide (ITO) (*41*–*44*). Sadekar *et al.* reported methods for covalently anchoring an EDOT vinyl derivative (3,4-vinylenedioxythiophene) onto free-radical initiator (azobisisobutyronitrile)–functionalized surfaces,

[1]Department of Materials Science and Engineering, University of Delaware, Newark, DE 19716, USA. [2]Department of Materials Science and Engineering, Pennsylvania State University, College Park, PA 16801, USA. [3]Department of Biomedical Engineering, University of Delaware, Newark, DE 19716, USA.
*Present address: Biomolecular and Organic Electronics, IFM, Linköping University, SE-581 83 Linköping, Sweden.
†Corresponding author. Email: milty@udel.edu

followed by chemical copolymerization with EDOT. The product was a highly adhesive PEDOT coating on these substrates (*45*).

Recently, electrografting has emerged as an effective strategy to significantly improve film adhesion by creating covalent chemical bonds between organic molecules and conducting solid substrates (*46*–*48*). The term "electrografting" describes a process in which an organic molecule is electrochemically oxidized or reduced, followed by the formation of metal-organic bonds at the substrate-polymer interface. The actual chemistry usually takes multiple steps. In general, an electron transfer process is involved (*46*). Electrografting stands out from other surface modification methods because of its high selectivity, efficiency, and versatility. The modification only happens on the conducting substrate where an external potential has been applied, making it possible to address small microelectrode surfaces or individual channels of patterned microelectrode arrays (*49*). Compared to the relatively slow SAM and silanization methods, surface modification through electrografting only takes several minutes. Furthermore, a variety of materials have been used as the conducting substrate, including gold, platinum, glassy carbon, stainless steel, nickel, silicon, and ITO (*46*, *47*, *50*).

The covalent bonds formed between the organic species and the substrate during electrografting have the advantage of having stronger bonding energies. Therefore, it is possible to create highly adherent conducting polymers on solid substrates with electrografting. For example, Jérôme's group (*51*) reported a two-step electrografting method to create chemisorbed conducting polythiophene or polypyrrole on a variety of substrates by first anchoring layers of methacrylate monomers. Further studies from this group demonstrated that these acrylate-modified surfaces supported the deposition of well-adherent poly(pyrrole-*co*-pyrrole-PEO) copolymers that were otherwise difficult to form because of the high solubility of the hydrophilic polyethylene oxide (PEO)–containing copolymer (*31*). In situ–generated pyrrole diazonium salt derivatives that were electrografted onto nickel surfaces were also reported (*52*). The resultant films had improved adhesion, although they served as a barrier to electrochemical transport (*52*). Oligothiophenes can also be grafted onto platinum and glassy carbon through similar means, forming a thin layer of an electroactive coating (*49*). Ouhib *et al.* (*53*) used this method to successfully graft poly(3-hexylthiophene) and polythiophene–polyethylene glycol/acrylate triblock copolymer micelles onto ITO substrates.

Here, we report a two-step approach to creating covalently bonded, strongly adherent, and highly conducting PEDOT films on metal and metal oxide (ITO) substrates. A methylamine-functionalized EDOT derivative, EDOT-NH_2 (*54*), was synthesized and used as the anchoring layer. As shown in Fig. 1, in the first step, EDOT-NH_2 was covalently bonded onto the substrate through the electrografting of the amine moieties. This resulted in the formation of a thin, cross-linked, nonconjugated, yet electrically transparent P(EDOT-NH_2)–based organic film on the substrate. The functional EDOT moieties in this film were then copolymerized with EDOT, forming a conjugated polymer that was covalently bonded on the substrates. The PEDOT film adhesion was greatly enhanced with this method. The chemical structure, electric properties, and morphology of the P(EDOT-NH_2) anchoring layer were investigated in detail.

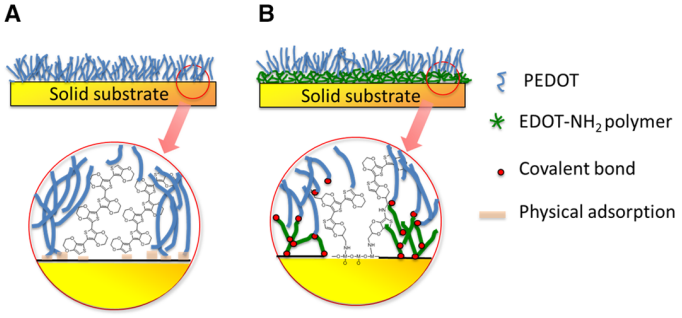

Fig. 1. Schematic representation of the adhesion-promoting layer. (**A**) PEDOT deposition on solid substrates. (**B**) PEDOT deposition on the electrografted P(EDOT-NH_2) layer.

RESULTS

The anodic potential scan of EDOT-NH_2 in acetonitrile solution is shown in Fig. 2. For platinum (Pt) electrodes, an oxidation current that initiated at +0.4 V and peaked at +1.1 V (versus Ag/AgCl) was found.

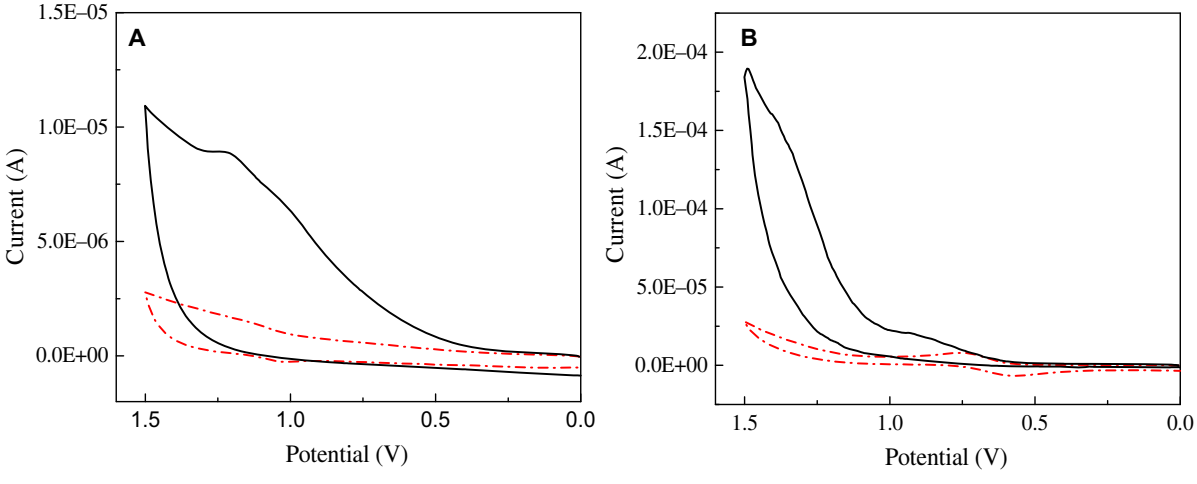

Fig. 2. Wide potential scan in EDOT-NH_2 solution. (**A**) Pt in EDOT-NH_2 acetonitrile solution with 0.1 M tetrabutylammonium perchlorate (TBAP) as electrolyte (black solid line); Pt in 0.1 M TBAP acetonitrile supporting electrolyte (red dashed line). (**B**) ITO in EDOT-NH_2 acetonitrile solution with 0.1 M TBAP as electrolyte (black solid line); ITO in 0.1 M TBAP acetonitrile supporting electrolyte (red dashed line). Potential was plotted against the Ag/AgCl pseudoreference electrode (–0.48 V versus ferrocene $E_{1/2}$).

For ITO, the corresponding peak positions were at +0.6 and +1.2 V, respectively. The shoulder in the peak suggests a two-electron transfer process, corresponding to the individual oxidations of the amine and EDOT moieties. It has been reported that the electrochemical oxidation of amines results in the immobilization of nitrogen-containing species onto a variety of substrates including carbon (*55*–*58*), platinum (*48*), gold (*59*), and ITO (*60*). As shown in Scheme 2, the proposed electrografting mechanism involves an electron transfer process through which an NH_2 radical cation is generated. The cation then loses a proton on the neighboring CH group, resulting in a radical that equilibrates between the CH and NH groups. Through the aminyl radical, the molecule forms a chemical bond with the substrate (*46*, *48*). Typically, the anodic peak current voltage for the reaction was found to be around +1 V versus Ag/AgCl, where primary amines show their largest reactivity (*48*, *56*). The EDOT oxidation potential is about +1.2 V in acetonitrile, which is slightly higher than that of the amine (~1.1 V). After introduction of the NH_2 functional group, these two oxidations (the EDOT thiophene ring and the NH_2 side group) may compete with each other. The radical cation may also react with the organic solvent, leading to insufficient deposition. In addition, when nonconjugated chemical structures were introduced, the rapid passivation of the substrate prevented the further deposition of the polymer (*51*, *61*). Other functionalized EDOT derivatives, such as EDOT-Br, EDOT-acid, and EDOT-OH, can be readily polymerized into their corresponding P(EDOT-Br), P(EDOT-acid), and P(EDOT-OH) polymers through electrochemical methods. However, we found that the electrochemical oxidation of EDOT-NH_2 in organic solutions or aqueous solution with organic dopants, such as polystyrene sulfonate (PSS) and tetrabutylammonium perchlorate, did not yield proper P(EDOT-NH_2) film deposition. A similar finding was reported by Sun *et al.* (*62*). Even in an EDOT-NH_2 and EDOT 1:1 (molar ratio) solution, uniform deposition could not be obtained.

We did find, however, that uniform films of P(EDOT-NH_2) could be reproducibly deposited in basic aqueous solutions (pH 9 to 10) of EDOT-NH_2 with an overpotential of ~2 to 3 V. As shown in Fig. 3, a white film formed on the substrate after the deposition. Unlike PEDOT films, the white P(EDOT-NH_2) films have high absorption in the visible spectra from 400 to 600 nm. They also show an absorption maximum around 900 nm (Fig. 3), probably due to polaron absorption. This white color and corresponding shifts in the UV-visible (UV-vis) spectra indicate that the usual conjugated backbone structure of PEDOT films has been significantly disrupted.

A comparison of the FTIR spectra of the EDOT monomer, the EDOT-NH_2 monomer, and the white P(EDOT-NH_2) coating is shown in Fig. 3C. First, the successful introduction of an NH_2 group on the EDOT monomer side chain was confirmed by twin peaks near 3400 to 3300 cm^{-1} that are characteristic for N–H stretching. In addition, a shoulder peak at 1660 cm^{-1} appeared in the EDOT-NH_2 monomer IR spectrum, which is consistent with primary amine N–H bending. The IR spectrum of EDOT-NH_2–modified ITO confirmed the existence of amine-containing species on the surface. The N–H stretching peaks around 3400 to 3300 cm^{-1} became broad absorption on EDOT-NH_2–modified ITO, as has been observed elsewhere (*48*), suggesting densely packed NH groups. In addition, a clear peak at 1650 cm^{-1} could be attributed to N–H deformation (*63*). Meanwhile, the 1580 cm^{-1} IR signal characteristic for C=C stretching was significantly reduced in P(EDOT-NH_2), which is likely a result of the EDOT-NH_2 radical reacting with the aromatic thiophene ring.

The surface composition of the P(EDOT-NH_2) film was further characterized with x-ray photoelectron spectroscopy (XPS). As shown in Fig. 4, a survey scan showed that during P(EDOT-NH_2) deposition, the original indium and tin signals disappeared and strong N 1s and S 2p peaks appeared on the surface. The main elemental components of the P(EDOT-NH_2) film were oxygen, nitrogen, carbon, and sulfur, which are consistent with the XPS study and confirmed that this polymer film was of the expected composition.

To test the solubility of the P(EDOT-NH_2) films, the modified ITO was immersed in acetonitrile, chloroform, and ethanol for 24 hours. It was found that these organic solvents could neither dissolve the film nor remove it from the solid substrate. In addition, we found that the P(EDOT-NH_2) film could not be removed by extended ultrasonication in water.

The morphology of P(EDOT-NH_2) films was observed with scanning electron microscopy (SEM). As shown in Fig. 5, at lower deposition charges (9 mC/cm^2), only a thin layer of film could be found on the ITO substrate. The grainy surface texture of the polycrystalline ITO was still visible under the film. With increased deposition charge

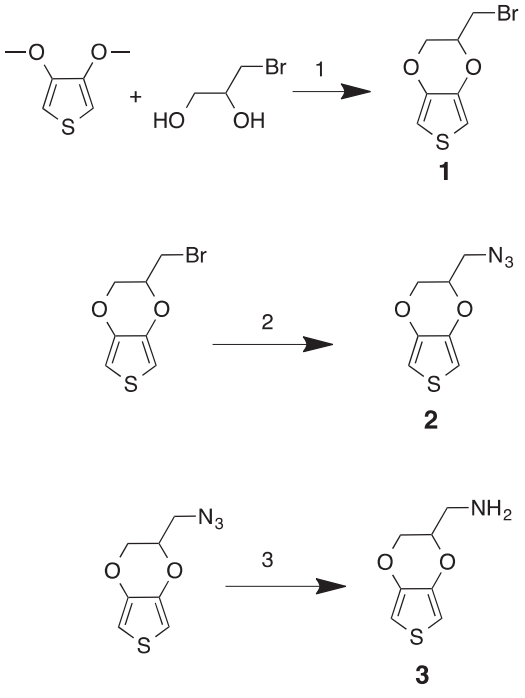

Scheme 1. Synthesis route of (2,3-dihydrothieno[3,4-b][1,4]dioxin-2-yl)methanamine (EDOT-NH_2). Conditions: 1: p-toluenesulfonic acid, toluene, 90°C, 16 hours. 2: NaN_3, DMF (N,N′-dimethylformamide), room temperature (RT), 17 hours. (*74*). 3: triphenylphosphine, NaOH, 50°C. (*54*).

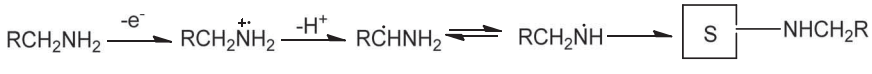

Scheme 2. Proposed electrografting mechanism of amines, adopted from Collazos-Castro *et al.* (*17*).

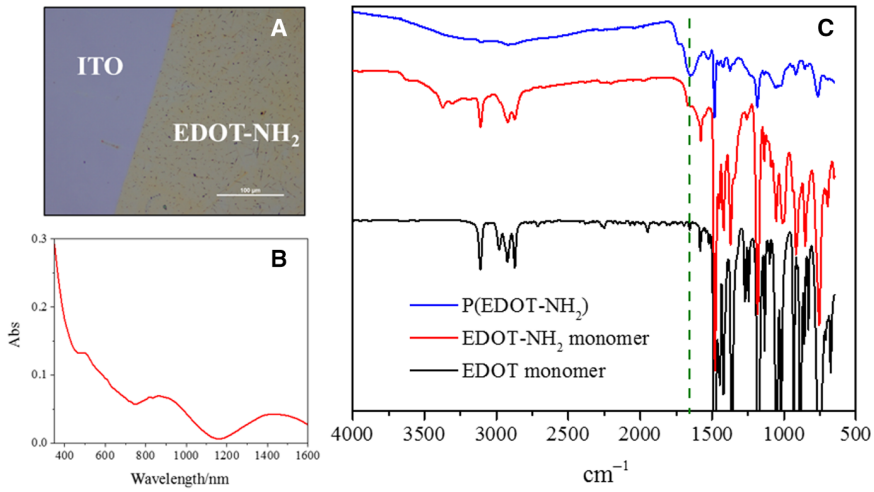

Fig. 3. P(EDOT-NH_2) film coated on ITO. (**A**) Optical micrograph of the film edge. (**B**) UV-vis–near-infrared (NIR) spectrum of the film. (**C**) Fourier transform IR (FTIR) spectra of the EDOT monomer, the EDOT-NH_2 monomer, and the P(EDOT-NH_2) film.

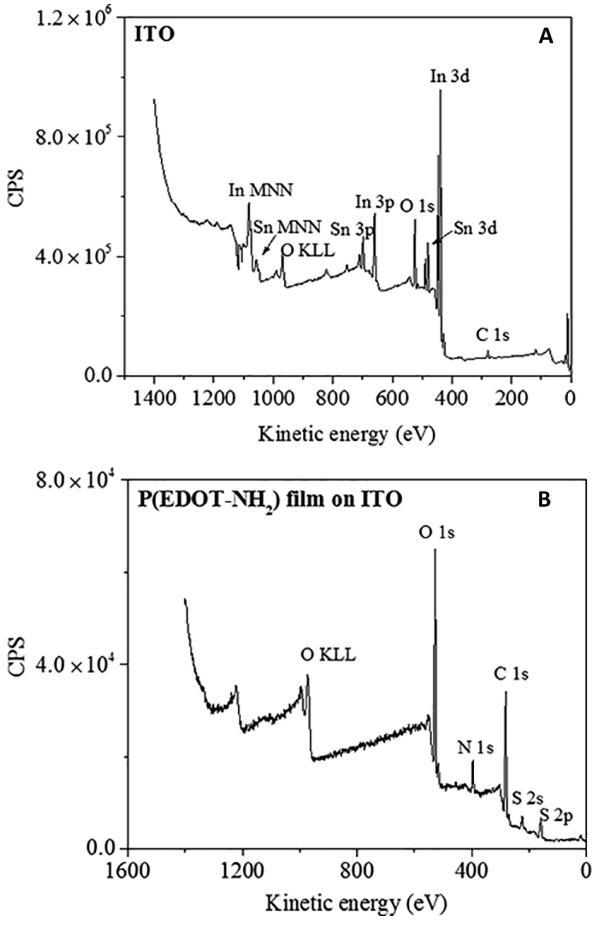

Fig. 4. XPS of (A) bare ITO and (B) EDOT-NH_2–coated ITO.

(72 mC/cm^2), thin bumpy layers were deposited on the substrate. Nanometer-sized pores were relatively uniformly distributed on the P(EDOT-NH_2) films. Further increases in the deposition charge led to a diminished density of the nanopores, resulting in a dense, bumpy, yet otherwise featureless film. A scratch test on the film obtained at a deposition charge of 72 mC/cm^2 revealed that the thickness of the film was around 1 μm (fig. S1A). In addition, focused ion beam (FIB)–SEM, used to study the cross section of the P(EDOT-NH_2) film, demonstrated that the film was highly sensitive to the gallium ion beam. As shown in fig. S1 (B and C), the surface layer of the film was quickly removed by the imaging beam, leaving an approximately 200-nm-thick residue. Multiple pores were distributed in the residue. These pores were similar in size to the bumps in the original film, which may suggest the underlying structure of the P(EDOT-NH_2) film on ITO.

The P(EDOT-NH_2) films were deposited on platinum microelectrodes with different deposition charges. As shown in Fig. 6, although an optically thick EDOT-NH_2 film was produced at a deposition charge of 72 mC/cm^2, the film did not significantly block the charge transport of the electrodes. From 36 to 144 mC/cm^2, the impedance amplitudes over 1 to 100 kHz of the modified platinum electrodes were essentially the same as those of the bare ones. For much thicker films (~288 mC/cm^2 charge and above), the impedance significantly increased at higher frequencies, indicating that the thick coating eventually hinders charge transport.

A comparison of the impedance amplitudes at the neurologically relevant temporal frequency of 1 kHz is shown in Fig. 6C. The impedance of EDOT-NH_2–modified electrodes at 1 kHz was similar to that of the bare electrode. At a higher deposition charge (576 mC/cm^2), the impedance increased from around 350 to 550 ohms. On the other hand, the deposition of EDOT-NH_2 on Pt electrodes slightly decreased the charge storage capacity (CSC) of the electrode. At 576 mC/cm^2, the CSC decreased from 3.05 ± 0.28 mC/cm^2 to 1.96 ± 0.35 mC/cm^2. This decrease in CSC shows that, unlike PEDOT, the EDOT-NH_2 films were not electroactive. However, both the impedance spectra and the cyclic voltammetry (CV) testing showed that, for sufficiently thin P(EDOT-NH_2) films, charge transport between electrode and the electrolyte was not significantly impeded.

The adherent P(EDOT-NH_2) coating provides an excellent anchor layer for subsequent PEDOT electrochemical polymerization. First, the same amount of charge was used to deposit PEDOT onto ITO substrates that were modified with P(EDOT-NH_2) films of different charges (thicknesses). As shown in fig. S2, uniform dark blue PEDOT films could be readily polymerized on the EDOT-NH_2 films. When PEDOT films deposited from a fixed deposition charge of 72 mC/cm^2 on to 9, 18 and 72 mC/cm^2 P(EDOT-NH_2) films respectively, all the films showed

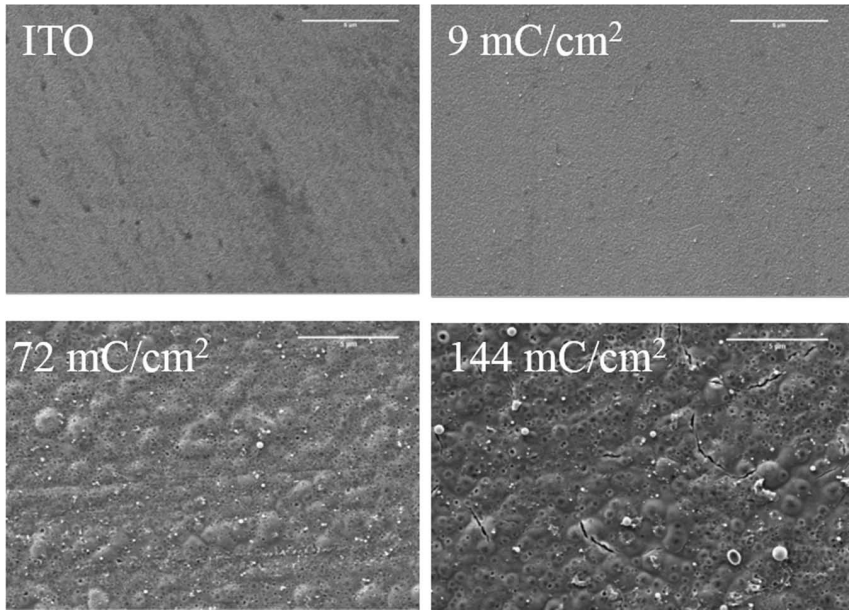

Fig. 5. SEM images of P(EDOT-NH_2) films deposited at different charge densities. Scale bars, 5 μm.

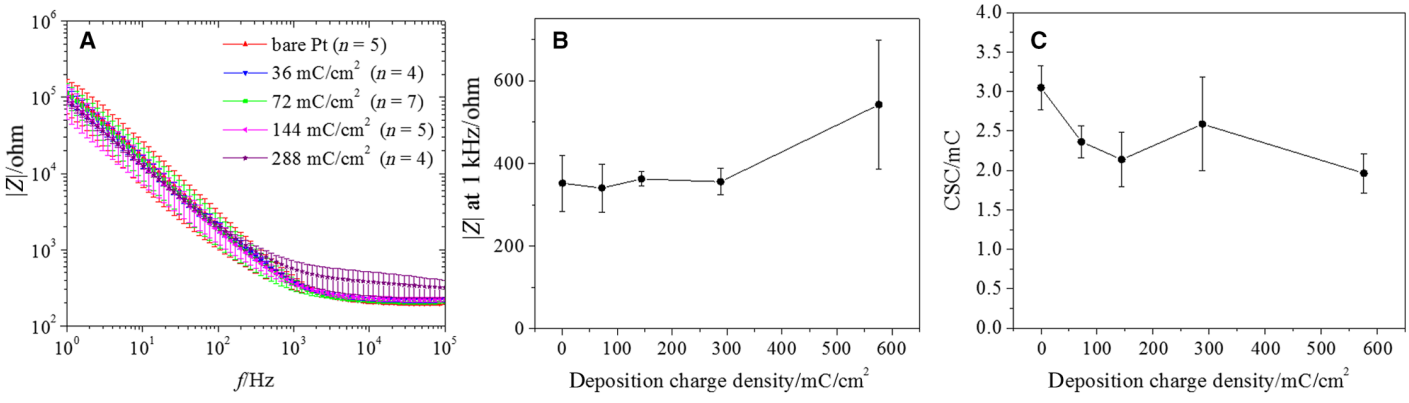

Fig. 6. Electroactivity of P(EDOT-NH_2) on platinum electrodes. (**A**) Impedance spectra of EDOT-NH_2 coatings at different deposition charge densities. (**B**) Impedance spectra of EDOT-NH_2 coatings at different depostion charge densities. (**C**) Charge storage capacity (CSC) of P(EDOT-NH_2) coating at different deposition charge densities.

similar blue colors. However, there seemed to be considerably less PEDOT deposition on the 144-mC/cm^2 P(EDOT-NH_2) film. The film became just slightly colored after PEDOT deposition at 72 mC/cm^2.

Next, PEDOT of various deposition charges was polymerized onto P(EDOT-NH_2) films prepared under the same deposition charge (72 mC/cm^2). As shown in Fig. 7, at a low PEDOT deposition charge (4 mC/cm^2), only a slight blue tone appeared on the surface. Closer examination under SEM showed that the film seemed to shrink first, leaving multiple pores on the surface. It is surmised that the volume shrinkage [possibly caused by the reaction between the EDOT monomer and EDOT moieties in the P(EDOT-NH_2) film, which became cross-linked] resulted in the collapse of the polymer network. At 9 mC/cm^2, the blue color became optically deeper. SEM images showed that both the pore size and density also increased. At 72 mC/cm^2, ~1-μm PEDOT bumps were found on the film. The density of these PEDOT bumps greatly increased at 144 mC/cm^2.

To evaluate the electrical properties of PEDOT deposited on P(EDOT-NH_2)–modified substrates, we used a 16-channel NeuroNexus "Michigan"-style neural probe with 413-$μm^2$ iridium recording electrodes. First, six recording electrodes were coated with P(EDOT-NH_2) films at a deposition charge of 1 C/cm^2. Consecutive PEDOT depositions at the same charge density were then performed. Bare electrodes and 1-C/cm^2 PEDOT–coated electrodes served as control groups. As shown in Fig. 8, the successful depositions were confirmed by a dark layer of film observed on the metal electrodes. These soft conducting coatings had large effective surface areas that markedly enhanced the charge transport of the electrodes. As shown in Fig. 8B, the PEDOT coatings decreased the impedance of the metal electrodes over the entire frequency spectrum. At lower frequencies, a two-order decrease of impedance amplitude was found. Although P(EDOT-NH_2) depositions were performed at the same deposition charge, the impedance of P(EDOT-NH_2)–modified electrodes was close to that of the bare electrodes. Another layer of PEDOT deposition at 1 C/cm^2 on the P(EDOT-NH_2)–modified electrodes, like PEDOT, decreased the impedance by one to two orders of magnitude. At 1 kHz, the impedance of the bare electrode was 304 ± 172 kilohms. P(EDOT-NH_2) modified electrodes had an impedance of 309 ± 41 kilohms. After

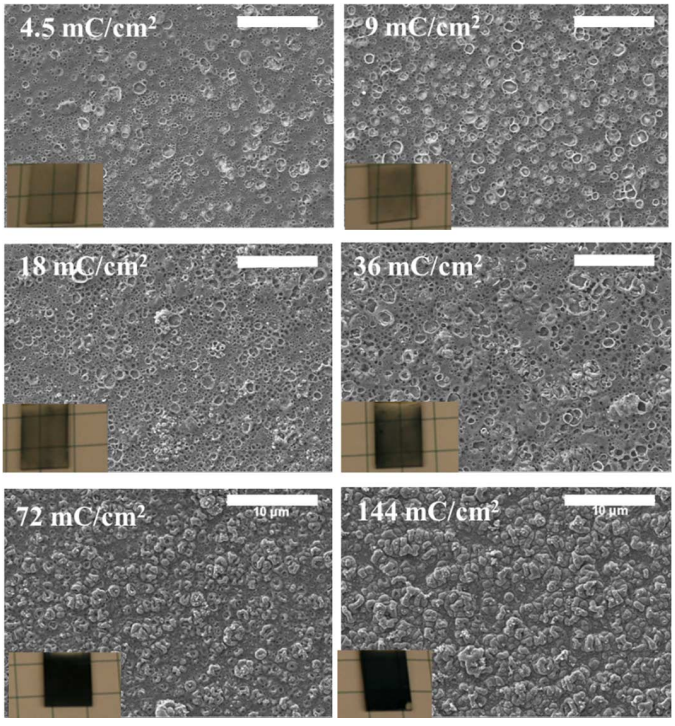

Fig. 7. SEM images of PEDOT of different deposition charge densities deposited on P(EDOT-NH_2) with the same deposition charge density (72 mC/cm^2). The insets show the optical image of the depositions on ITO (7 mm wide). Scale bars, 10 μm.

coating with PEDOT, the impedance of bare Ir electrodes dropped to 20 ± 4 kilohms, while that of EDOT-NH_2–modified electrodes was 17 ± 5 kilohms. Because impedance magnitude is also a function of electrode area, we normalized the impedance magnitude by defining the surface normalized value $Z' = Z{\cdot}A$, where Z is the measured impedance amplitude at a given frequency and A is the electrode area. At 1 kHz, the surface normalized impedance for bare Ir, P(EDOT-NH_2) film–modified Ir, PEDOT on Ir, and PEDOT on P(EDOT-NH_2)–modified Ir was calculated to be 1.26×10^8, 1.28×10^8, 8.26×10^6, and 7.02×10^6 ohms μm^2, respectively.

PEDOT coatings greatly improved the CSC of the bare electrodes as well. As shown in Fig. 8D, when compared to the bare electrodes, the CV of bare electrodes showed a large capacitance. The CSC of the bare electrodes was found to be 0.91 ± 0.23 mC/cm^2. PEDOT increased the CSC of the system to 6.72 ± 0.74 mC/cm^2. PEDOT on P(EDOT-NH_2)–modified electrodes showed a comparable CSC of 7.85 ± 0.44 mC/cm^2.

This electrochemical stability of PEDOT on the P(EDOT-NH_2) film was evaluated with CV. As shown in Fig. 9, 300 cycles of CV between −0.6 and +0.8 V were performed on PEDOT grown on P(EDOT-NH_2)–modified ITO. It was found that the impedance increased after each CV cycling. Initially, the impedance at 1 Hz dropped from ~2000 ohms (1.0×10^{11} ohms μm^2) for P(EDOT-NH_2)–modified ITO to ~100 ohms (0.5×10^9 ohms μm^2) after PEDOT deposition. After 100, 200, and 300 cycles of CV, it increased to ~200, ~600, and ~800 ohms, respectively. Accompanying the decrease in conductivity was a corresponding decrease in CSC. As shown in Fig. 9 (right), the integrated area during CV decreased considerably after the first 100 cycles. It continued to decrease during consecutive sweepings, which suggests some loss of conducting material from the electrode surface.

The adhesion of PEDOT/P(EDOT-NH_2) coatings on ITO was evaluated in an aggressive mechanical test. The film on ITO was subjected to sonication at 25°C for 1 hour. As shown in Fig. 10, only minimal material loss was found on the ITO substrate, while PEDOT alone on ITO quickly dissipated under sonication after just 5 s. These results strongly indicate that electrografting of P(EDOT-NH_2) is a powerful method to create highly adherent, covalently bonded coatings of PEDOT on the metal and metal oxide substrates.

DISCUSSION

The goal of this study was to create strongly adherent PEDOT coatings on inorganic solid conducting substrates via a two-step reaction. First, an EDOT derivative, EDOT-NH_2, was deposited into a cross-linked, adherent, electron-transparent P(EDOT-NH_2) thin film on the electrode surface using electrografting. Second, PEDOT was polymerized on the P(EDOT-NH_2)–modified electrodes to form electrically active films that were strongly mechanically anchored to the surface through the P(EDOT-NH_2) adhesion layer.

It is worth mentioning that the spontaneous absorption of amines on metal and glassy carbon surfaces was clearly demonstrated only recently, by Gallardo *et al.* (*63*). There was also evidence that this absorption was through a chemical bond formed between the metal and the nitrogen. A wide range of amines can form this kind of adsorption. However, it is a relatively slow process, and it is unlikely that more than a monolayer of coating would be deposited.

On the other hand, the electrografting of amines provides an efficient route to covalently anchor organic molecules onto a variety of conducting substrates with adequate surface coverage. Electrografting can be performed at relatively low oxidation potentials, and the reaction is quick (*64*). The electrografting of the amine competes with the oxidation of EDOT. Because the EDOT oxidation requires a slightly higher oxidation potential of +1.2 V, the electrografting of the amine will predominate. This conclusion is supported by our observation that the deposited polymers only showed evidence for limited backbone conjugation in UV-vis spectroscopy and showed a white color.

White P(EDOT-NH_2) films (with a thickness of up to 1 μm) were deposited by electrochemically oxidizing EDOT-NH_2 from aqueous solutions under slightly basic conditions. The P(EDOT-NH_2) film was likely anchored directly onto the substrate via covalent bonds, as was evident from the fact that neither organic solvents nor ultrasonication could remove the film. The composition of oxygen, sulfur, carbon, and nitrogen was confirmed by XPS. The presence of NH_2 and C=C bonds was verified by FTIR spectroscopy.

Amine films generated through electrografting methods are usually restricted to monolayer or nanometer thicknesses (*48*, *56*, *65*) because of the high impedance of the electrode after initial deposition (passivation) (*66*). The micrometer-range thickness of these P(EDOT-NH_2) films indicates that the material can be deposited well beyond a monolayer. Therefore, a cross-linked polymer multilayered network is a better description of its overall chemical structure.

Multilayer structures for electrografted polymers have been previously described, such as in the case of aryl diazonium electrografting (*67*). A proposed mechanism was that, under the reducing current, aryl radicals were generated (*68*). These radicals could either attach onto the substrate through organic-metal covalent bonds or react with already bonded species, forming a polymer network (*48*, *68*). Still, the polymer films in this previous study were nominally only 20 to 30 nm thick (*69*), possibly due to their highly insulating nature. The passivation of electrodes was confirmed by the general current decrease after the first voltammogram scan. It was also supported by the marked impedance

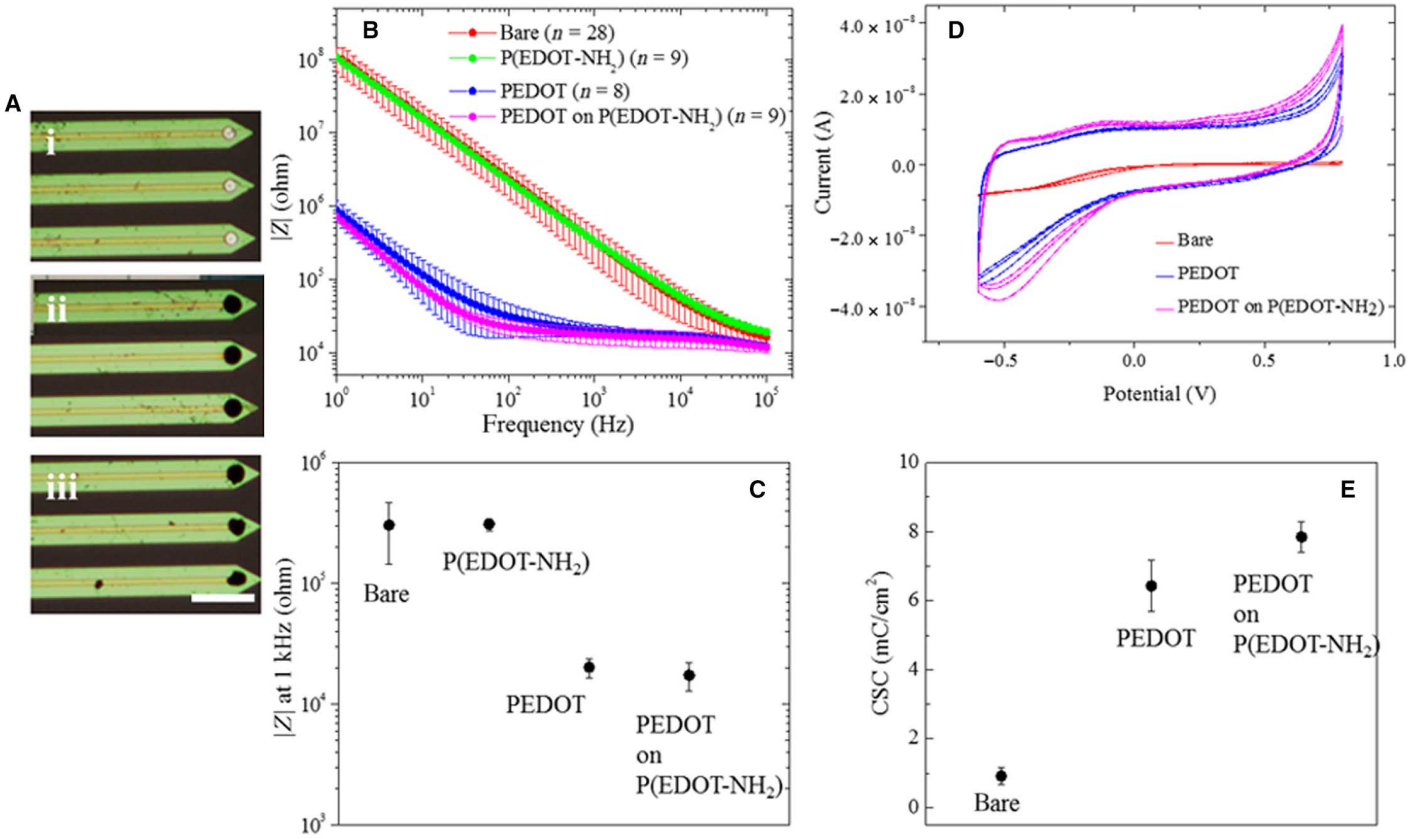

Fig. 8. PEDOT and PEDOT-P(EDOT-NH_2) depositions on microelectrodes. (**A**) Optical micrograph of (i) bare NeuroNexus electrodes, (ii) PEDOT-coated electrodes, and (iii) PEDOT on EDOT-NH_2–modified electrodes. Scale bar, 100 μm. (**B**) Average impedance spectra of PEDOT, P(EDOT-NH_2), PEDOT on P(EDOT-NH_2), and bare electrodes. (**C**) Impedance magnitude at 1 kHz of the three polymer coatings and the bare electrodes. (**D**) CV of PEDOT, PEODT on P(EDOT-NH_2), and bare electrodes. (**E**) CSC of PEDOT, PEDOT on P(EDOT-NH_2), and bare electrodes.

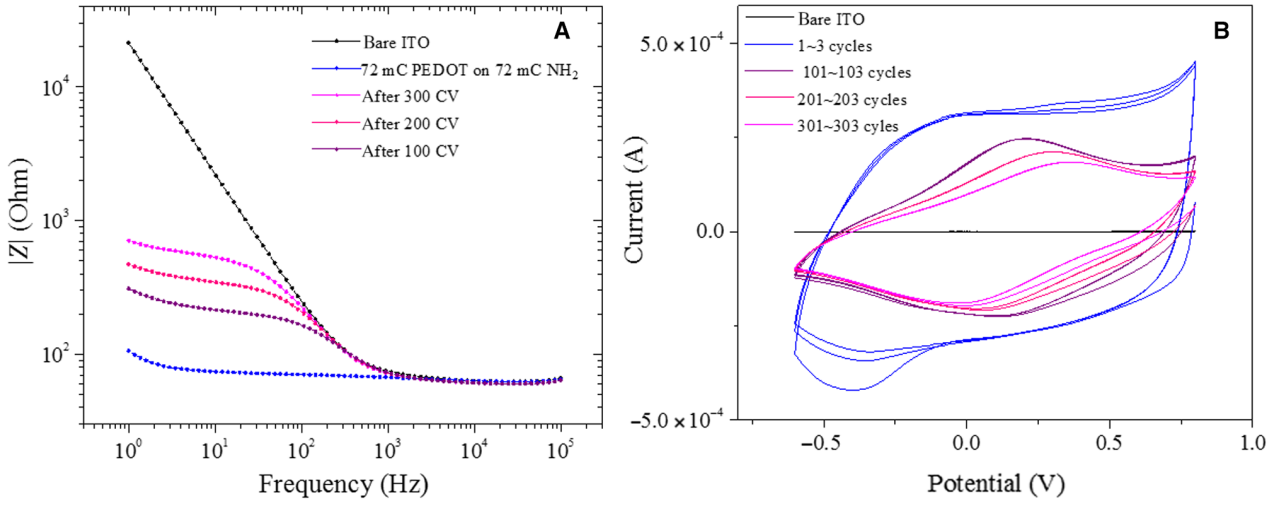

Fig. 9. Electrochemical stability of PEDOT on P(EDOT-NH_2). (**A**) Impedance spectra of 72-mC/cm^2 PEDOT on 72-mC/cm^2 P(EDOT-NH_2)–coated ITO before and after 100, 200, and 300 cycles of CV scans. (**B**) CV changes during scanning.

increase after electrografting. For example, 240 s of 4-nitrophenyldiazonium electroreduction on glass carbon increased the charge transfer resistance of the substrate from 422 to 1.3 × 10^6 ohms (*70*). Because the charge transport of the system was blocked by the insulating film, less organic molecules in the solvent could be subsequently activated. As a result, the growth of multilayer film was limited. When the grafting mechanism allows the formation of a conjugated polymer multilayer, the blocking effect was mitigated. Much thicker films can then be formed (*71*).

Multilayer structures in the amine electrografting have been even less intensively studied. Buriez *et al.* described a multilayer deposition mechanism of pi-conjugated amino-ferrocifen, in which the activated amine radicals in the solution were added to already grafted molecules,

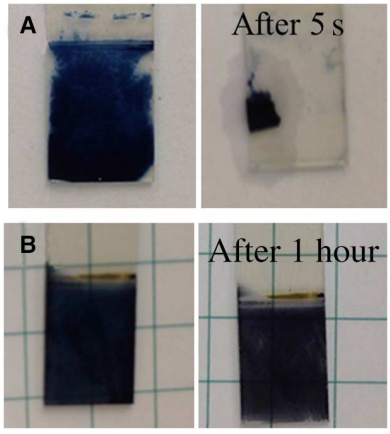

Fig. 10. Ultrasonication tests on PEDOT films. (**A**) PEDOT coating on ITO before (left) and after (right) 5 s of ultrasonication. (**B**) PEDOT on P(EDOT-NH_2)–modified ITO before (left) and after (right) 1 hour of ultrasonication. The width of the ITO glass slides is 0.7 cm.

similar to aryl network formation from reduced aryl diazonium. In their case, potentiostatic depositions at 0.9 V for 30 min produced films with a thickness of 85 ± 7.0 nm (*59*). The limiting factor of the film growth could still be the quick passivation of the electrode. Bardini *et al.* found that an approximately 10-nm electrografted allylamine was enough to induce a huge charge transfer resistance (*66*). However, thick nonconjugated polyethylenimine coatings (~30 μm) on p-Si were reported by Herlem *et al.* (*72*). In their method, high overpotential (0 to +10 V) voltammogram scans were used to produce thick films. Despite the film obtained from the first scan, the passivation of the electrodes was still evident from the rapid drop of current response at the second voltammogram scan.

The EDOT-NH_2 electrografting used to form P(EDOT-NH_2) under galvanostatic conditions studied here is likely to follow a similar mechanism. The EDOT aminyl radicals are generated first. These radicals would be anchored onto the conducting substrates. The further activated radicals in the solution coupled onto the EDOT moieties on the grafted molecules, forming the nonconjugated, cross-linked P(EDOT-NH_2) polymer. Continued film growth requires sufficient charge transport to oxidize the EDOT-NH_2 molecules in the solution, which is infeasible for a passivized electrode. Two sources may provide the necessary charge transport through the film to the monomer solutions. First, electrografting was not uniform on the substrate. During the multilayer growth, pinholes were formed, which allowed for sufficient charge transport. Because there are competing reactions between the EDOT oxidation and NH_2 oxidation, the conjugated P(EDOT-NH_2) polymer or oligomers may also be formed. In the polymer matrix, these conjugated polymers may serve as "molecular wires" for the charge conduction through the film. The real structure is likely a complex hybrid polymeric film.

Impedance spectra demonstrated that the electrografted P(EDOT-NH_2) film allowed sufficient charge transport because the modified electrodes had nearly identical impedance spectra with the bare substrates. Only at a much higher deposition charge was a slight increase of impedance found. Because they are not insulating to the substrate, the P(EDOT-NH_2) films are a suitable adhesion-promoting layer for the electrochemically deposited PEDOT.

The strong attachment of the electrografted P(EDOT-NH_2) layer to the substrate supports the assertion that covalent bonds exist between them (*46*). It was found that PEDOT could grow on the P(EDOT-NH_2) films of various thicknesses. Optically denser PEDOT depositions were found on relatively thinner P(EDOT-NH_2) films, suggesting that thicker P(EDOT-NH_2) coatings might not support efficient PEDOT growth. At low deposition charge densities, holes were found on P(EDOT-NH_2) films, which may be a result of film shrinkage induced by the polymerization of the EDOT moieties. PEDOT particles growing inside the holes and on the P(EDOT-NH_2) film were observed. The result was a bumpy PEDOT morphology anchored on the ITO substrate. PEDOT deposited on the P(EDOT-NH_2)–modified microelectrode had similar low impedance to PEDOT on unmodified electrodes.

Repeated charge injection is required for chronic neural stimulations, a fact that poses problems for the mechanical stability of conducting polymer coatings: During charge injection, the polymers are reduced and oxidized, leading to conformational changes of the polymer chain as well as dopants dissociating and associating with the polymer matrix. Volume changes have also been observed (*73*). The possibility of overoxidation under high voltage may also cause polymer degradation. Both processes likely contribute to the delamination and cracking of the polymer material. We found moderate electrochemical stability of the PEDOT growing on P(EDOT-NH_2)–modified ITO. The loss of materials under CV cycling was evident from electrochemical impedance spectroscopy (EIS) and the integrated area of the CV curve. However, when compared to PEDOT coatings on bare ITO, which became delaminated as a "freestanding" film after 300 cycles of CV, P(EDOT-NH_2) coatings provided significantly improved mechanical stability.

An aggressive mechanical test was performed on PEDOT and PEDOT on P(EDOT-NH_2) films by subjecting them to ultrasonication. The superior adhesion of the P(EDOT-NH_2) became immediately obvious because the PEDOT on ITO [without P(EDOT-NH_2)] was shattered after only 5 s of sonication, whereas PEDOT on P(EDOT-NH_2) films remained relatively intact after 1 hour. This test again indicates that there were covalent bonds formed between the P(EDOT-NH_2) anchoring layer and the substrate as well as the P(EDOT-NH_2) anchoring layer and PEDOT.

CONCLUSIONS

We designed and evaluated a method of electrochemically grafting a P(EDOT-NH_2) polymer onto conducting solid substrates, such as platinum, iridium, and ITO. The nonconjugated, cross-linked polymer film was insoluble in common organic solvents and was extremely adherent to the inorganic substrate. XPS showed that the P(EDOT-NH_2) contains the nitrogen, carbon, and sulfur expected from its chemical composition. FTIR spectra revealed a chemical structure similar to the EDOT-NH_2 monomers. The formation of the P(EDOT-NH_2) polymer presumably occurred through the addition of activated aminyl radicals with the thiophene rings of already anchored EDOT-NH_2 molecules. When coated on the conducting substrates, the polymer sufficiently covered the surface of these substrates. Although the P(EDOT-NH_2) films can be grown into micrometer-thick layers, they did not significantly block (or enhance) the charge transport of the system. Subsequent PEDOT polymerization was performed on P(EDOT-NH_2)–modified substrates. The end result was highly conducting and strongly adherent conducting polymer films on either metals or metal oxides.

MATERIALS AND METHODS

Chemical synthesis

For the synthesis of EDOT-Br (**1**), 3,4-dimethoxythiophene (3.2 g, 22 mmol; Sigma-Aldrich) was dissolved in 15 ml of dry toluene in a

three-neck flask equipped with a stir bar. *p*-Toluenesulfonic acid monohydrate (0.15 g; Sigma-Aldrich) was added into the solution. The temperature was increased to 90°C. Under reflex and the protection of argon, 4.9 g (31 mmol) of 3-bromo-1,2-propanediol in 15 ml of toluene solution was added dropwise through an additional funnel. After addition, the mixture was allowed to react for 16 hours at 90°C before another 4.9 g of 3-bromo-1,2-propanediol in 15 ml of toluene was added. It was allowed to react for another 3 hours. The mixture was cooled down to RT. The solvent was removed by rotary evaporation, and the solids were redissolved in chloroform. It was washed three times with saturated $NaHCO_3$ solution (Thermo Fisher Scientific), followed by washing three times with deionized (DI) water. The organic layer was dried under $MgSO_4$ (Thermo Fisher Scientific). After filtration, the solvent was removed by rotary evaporation. The product was purified with chromatography (eluent: dichloromethane/hexane, 3:2). ^{1}H NMR (400 MHz, $CDCl^3$): δ = 6.40-6.38 (dd, ^4J = 4.0 Hz, 2H, S-CH); 4.5-4.1 (m, 3H, O-CH_2-CH-O); 3.6-3.5 (m, 2H, CH^2-Br). ^{13}C NMR (100 MHz, $CDCl_3$): δ =141.1; 140.7; 100.2; 72.6; 66.2; 28.6.

For the synthesis of EDOT-N_3 (**2**), the procedure was adopted from Daugaard *et al.* (*74*). Briefly, 0.22 g (0.9 mmol) of **1** was dissolved in 10 ml of DMF in a round-bottom flask equipped with a stir bar. NaN_3 (0.08 g, 1.2 mmol; Thermo Fisher Scientific) was then added. The mixture was stirred at RT for 17 hours. It was then diluted in 15 ml of DI water. The mixture was then extracted five times with ethyl acetate (Thermo Fisher Scientific). The organic layer was washed three times with DI water and once with brine. It was dried against $MaSO_4$ (Thermo Fisher Scientific). The solvent was removed by rotary evaporation. The product was slightly yellow oil. ^{1}H NMR (400 MHz, $CDCl_3$): δ = 6.42/6.38 (dd, ^4J = 4.0 Hz, 2H, S-CH); 4.4-4.0 (m, 3H, O-CH_2-CH-O); 3.7-3.5 (m, 2H, CH_2-N_3). ^{13}C NMR (100 MHz, $CDCl_3$): δ = 141.1; 140.7; 100.3; 100.2; 72.5; 65.8; 50.5.

For the synthesis of EDOT-NH_2 (**3**), the procedure was adopted from Tansil *et al.* (*54*). In a two-neck flask that was equipped with a condenser and a stir bar, 1.43 g (7.2 mmol) of **2** was dissolved in 25 ml of tetrahydrofuran (THF) (Sigma-Aldrich). Protected under argon, 2.08 g (7.9 mmol) of triphenylphosphine was added. The system was heated at 50°C and allowed to react for 1 hour before 25 ml of 2 M NaOH was added. After reacting at 50°C for another 2 hours, the reaction mixture was cooled down to RT. Concentrated HCl was slowly added until the pH value was smaller than 3. THF was removed by rotary evaporation. The mixture was washed three times with dichloromethane. The aqueous layer was then adjusted to pH >10 with 2 M NaOH solution. The mixture was extracted three times with dichloromethane. The organic layer was combined and dried against $MgSO_4$ and dried under rotary evaporation. The product was yellowish oil. ^{1}H NMR (400 MHz, $CDCl_3$): δ = 6.36/6.34 (dd, ^4J = 4.0 Hz, 2H, S-CH); 4.25-4.0 (m, 3H, O-CH_2-CH-O); 3.0-2.9 (m, 2H, CH_2-N), 1.5 (broad s, 2H, NH_2). ^{13}C NMR (100 MHz, $CDCl_3$): δ = 141.7; 141.6; 100.0; 99.6; 75.2; 66.6; 42.3.

Electrochemical depositions

The electrografting and electrochemical depositions were performed on an Autolab PGstat12 Potentiostat/Galvanostat (Eco Chemie) in a glass cell equipped with a platinum wire as the counter electrode. The electrografting of EDOT-NH_2 films was performed in slightly basic EDOT-NH_2 aqueous solutions (0.02 M aqueous solution, pH 9 or 10). The electrochemical deposition of PEDOT was performed in 0.01 M EDOT with 0.02 M PSS (Sigma-Aldrich) as counter ion. Pt microelectrodes (0.02 cm^2; Bioanalytical Systems Inc.), ITO glass (0.5 cm^2; Delta Technologies), or 16-channel NeuroNexus A style electrodes (Ir, 144 μm^2) were used as working electrodes. For electrografting, a current density of 40 $\mu A/cm^2$ was used. For electrochemical depositions, a current density of 80 $\mu A/cm^2$ was used.

Characterization

CV characterizations of polymer films were performed on the same Autolab PGstat12 Potentiostat/Galvanostat. The tests were performed in 1× monomer-free phosphate buffered saline (PBS) solution with an Ag/AgCl glass body electrode (Thermo Fisher Scientific) as the reference. The scan rate was 100 mV/s.

EIS was performed in an electrochemical cell installed with a platinum foil as the counter electrode. Monomer-free PBS was used as the electrolyte. The same Autolab was used. For EIS measurement, a bias of 0.01 V versus Ag/AgCl was applied. The frequency range between 1 and 100 kHz was scanned. Attenuated total reflectance FTIR (ATR-FTIR) spectroscopy was performed on a PerkinElmer Spectrum 100 ATR-FTIR spectrometer. UV-vis-NIR spectra were collected on a Shimadzu UV-3600 UV-VIS-NIR spectrophotometer.

FIB-SEM was performed on an Auriga 60 CrossBeam FIB-SEM (Carl Zeiss). For SEM imaging, an acceleration voltage of 3 kV was used. For FIB milling, a 20-pA gallium ion beam was applied.

SUPPLEMENTARY MATERIALS

Supplementary material for this article is available at http://advances.sciencemag.org/cgi/content/full/3/3/e1600448/DC1

fig. S1. Cross section of P(EDOT-NH_2) deposited on ITO.

fig. S2. PEDOT deposition at 72 mC/cm^2 on P(EDOT-NH_2) anchoring layers that have different thicknesses.

fig. S3. Scratch tests on PEDOT on ITO and PEDOT on P(EDOT-NH_2)–modified ITO surface.

REFERENCES AND NOTES

1. Y. Xia, K. Sun, J. Ouyang, Solution-processed metallic conducting polymer films as transparent electrode of optoelectronic devices. *Adv. Mater.* **24**, 2436–2440 (2012).
2. M. V. Fabretto, D. R. Evans, M. Mueller, K. Zuber, P. Hojati-Talemi, R. D. Short, G. G. Wallace, P. J. Murphy, Polymeric material with metal-like conductivity for next generation organic electronic devices. *Chem. Mater.* **24**, 3998–4003 (2012).
3. K. Sun, S. Zhang, P. Li, Y. Xia, X. Zhang, D. Du, F. H. Isikgor, J. Ouyang, Review on application of PEDOTs and PEDOT:PSS in energy conversion and storage devices. *J. Mater. Sci.* **26**, 4438–4462 (2015).
4. L. Ouyang, C. L. Shaw, C.-c. Kuo, A. L. Griffin, D. C. Martin, In vivo polymerization of poly(3,4-ethylenedioxythiophene) in the living rat hippocampus does not cause a significant loss of performance in a delayed alternation task. *J. Neural Eng.* **11**, 026005 (2014).
5. S. E. Moulton, M. J. Higgins, R. M. I. Kapsa, G. G. Wallace, Organic bionics: A new dimension in neural communications. *Adv. Funct. Mater.* **22**, 2003–2014 (2012).
6. P. Gkoupidenis, N. Schaefer, B. Garlan, G. G. Malliaras, Neuromorphic functions in PEDOT:PSS organic electrochemical transistors. *Adv. Mater.* **27**, 7176–7180 (2015).
7. R. Green, M. R. Abidian, Conducting polymers for neural prosthetic and neural interface applications. *Adv. Mater.* **27**, 7620–7637 (2015).
8. D. Khodagholy, J. N. Gelinas, T. Thesen, W. Doyle, O. Devinsky, G. G. Malliaras, G. Buzsáki, NeuroGrid: Recording action potentials from the surface of the brain. *Nat. Neurosci.* **18**, 310–315 (2015).
9. A. Williamson, J. Rivnay, L. Kergoat, A. Jonsson, S. Inal, I. Uguz, M. Ferro, A. Ivanov, T. A. Sjöström, D. T. Simon, M. Berggren, G. G. Malliaras, C. Bernard, Controlling epileptiform activity with organic electronic ion pumps. *Adv. Mater.* **27**, 3138–3144 (2015).
10. D. C. Martin, G. G. Malliaras, Interfacing electronic and ionic charge transport in bioelectronics. *ChemElectroChem* **3**, 686–688 (2016).
11. S. J. Wilks, S. M. Richardson-Burns, J. L. Hendricks, D. C. Martin, K. J. Otto, Poly(3,4-ethylenedioxythiophene) as a micro-neural interface material for electrostimulation. *Front. Neuroeng.* **2**, 7 (2009).

12. K. A. Ludwig, J. D. Uram, J. Yang, D. C. Martin, D. R. Kipke, Chronic neural recordings using silicon microelectrode arrays electrochemically deposited with a poly(3,4-ethylenedioxythiophene) (PEDOT) film. *J. Neural Eng.* **3**, 59–70 (2006).
13. P. Fattahi, G. Yang, G. Kim, M. R. Abidian, A review of organic and inorganic biomaterials for neural interfaces. *Adv. Mater.* **26**, 1846–1885 (2014).
14. M. R. Abidian, D. C. Martin, Multifunctional nanobiomaterials for neural interfaces. *Adv. Funct. Mater.* **19**, 573–585 (2009).
15. H. Zhao, B. Zhu, S.-C. Luo, H.-A. Lin, A. Nakao, Y. Yamashita, H.-h. Yu, Controlled protein absorption and cell adhesion on polymer-brush-grafted poly(3,4-ethylenedioxythiophene) films. *ACS Appl. Mater. Interfaces* **5**, 4536–4543 (2013).
16. D. C. Martin, Molecular design, synthesis, and characterization of conjugated polymers for interfacing electronic biomedical devices with living tissue. *MRS Commun.* **5**, 131–153 (2015).
17. J. E. Collazos-Castro, G. R. Hernández-Labrado, J. L. Polo, C. García-Rama, N-Cadherin- and L1-functionalised conducting polymers for synergistic stimulation and guidance of neural cell growth. *Biomaterials* **34**, 3603–3617 (2013).
18. A. Alves-Sampaio, C. García-Rama, J. E. Collazos-Castro, Biofunctionalized PEDOT-coated microfibers for the treatment of spinal cord injury. *Biomaterials* **89**, 98–113 (2016).
19. M. R. Abidian, J. M. Corey, D. R. Kipke, D. C. Martin, Conducting-polymer nanotubes improve electrical properties, mechanical adhesion, neural attachment, and neurite outgrowth of neural electrodes. *Small* **6**, 421–429 (2010).
20. L. M. Do, E. M. Han, Y. Niidome, M. Fujihara, T. Kanno, S. Yoshida, A. Maeda, A. J. Ikushima, Observation of degradation processes of Al electrodes in organic electroluminescence devices by electroluminescence microscopy, atomic force microscopy, scanning electron microscopy, and Auger electron spectroscopy. *J. Appl. Phys.* **76**, 5118–5121 (1994).
21. S. G. Im, P. J. Yoo, P. T. Hammond, K. K. Gleason, Grafted conducting polymer films for nano-patterning onto various organic and inorganic substrates by oxidative chemical vapor deposition. *Adv. Mater.* **19**, 2863–2867 (2007).
22. S. R. Dupont, M. Oliver, F. C. Krebs, R. H. Dauskardt, Interlayer adhesion in roll-to-roll processed flexible inverted polymer solar cells. *Sol. Energy Mater. Sol. Cells* **97**, 171–175 (2012).
23. X. T. Cui, D. D. Zhou, Poly (3,4-ethylenedioxythiophene) for chronic neural stimulation. *IEEE Trans. Neural Syst. Rehabil. Eng.* **15**, 502–508 (2007).
24. R. Gerwig, K. Fuchsberger, B. Schroeppel, G. S. Link, G. Heusel, U. Kraushaar, W. Schuhmann, A. Stett, M. Stelzle, PEDOT–CNT composite microelectrodes for recording and electrostimulation applications: Fabrication, morphology, and electrical properties. *Front. Neuroeng.* **5**, 8 (2012).
25. C.-K. Cho, W.-J. Hwang, K. Eun, S.-H. Choa, S.-I. Na, H.-K. Kim, Mechanical flexibility of transparent PEDOT:PSS electrodes prepared by gravure printing for flexible organic solar cells. *Sol. Energy Mater. Sol. Cells* **95**, 3269–3275 (2011).
26. R. A. Green, R. T. Hassarati, L. Bouchinet, C. S. Lee, G. L. M. Cheong, J. F. Yu, C. W. Dodds, G. J. Suaning, L. A. Poole-Warren, N. H. Lovell, Substrate dependent stability of conducting polymer coatings on medical electrodes. *Biomaterials* **33**, 5875–5886 (2012).
27. T. A. Kung, N. B. Langhals, D. C. Martin, P. J. Johnson, P. S. Cederna, M. G. Urbanchek, Regenerative peripheral nerve interface viability and signal transduction with an implanted electrode. *Plast. Reconstr. Surg.* **133**, 1380–1394 (2014).
28. C. M. Frost, B. Wei, Z. Baghmanli, P. S. Cederna, M. G. Urbanchek, PEDOT electrochemical polymerization improves electrode fidelity and sensitivity. *Plast. Reconstr. Surg.* **129**, 933–942 (2012).
29. L. Ouyang, C.-c. Kuo, B. Farrell, S. Pathak, B. Wei, J. Qu, D. C. Martin, Poly[3,4-ethylene dioxythiophene (EDOT)-*co*-1,3,5-tri[2-(3,4-ethylene dioxythienyl)]-benzene (EPh)] copolymers (PEDOT-*co*-EPh): Optical, electrochemical and mechanical properties. *J. Mater. Chem. B* **3**, 5010–5020 (2015).
30. L. K. Povlich, J. C. Cho, S. Spanninga, D. C. Martin, J. Kim, Carboxylic acid-modified EDOT for bio-functionalization of neural probe electrodes. *Polymer Prepr.* **48**, 7–8 (2007).
31. S. Gabriel, M. Cécius, K. Fleury-Frenette, D. Cossement, M. Hecq, N. Ruth, R. Jérôme, C. Jérôme, Synthesis of adherent hydrophilic polypyrrole coatings onto (semi)conducting surfaces. *Chem. Mater.* **19**, 2364–2371 (2007).
32. H.-Y. Lee, J. Qu, Microstructure, adhesion strength and failure path at a polymer/roughened metal interface. *J. Adhes. Sci. Technol.* **17**, 195–215 (2003).
33. X. Cui, D. C. Martin, Fuzzy gold electrodes for lowering impedance and improving adhesion with electrodeposited conducting polymer films. *Sens. Actuators A Phys.* **103**, 384–394 (2003).
34. Z. Huang, P.-C. Wang, A. G. MacDiarmid, Y. Xia, G. Whitesides, Selective deposition of conducting polymers on hydroxyl-terminated surfaces with printed monolayers of alkylsiloxanes as templates. *Langmuir* **13**, 6480–6484 (1997).
35. K. S. Lee, G. B. Blanchet, F. Gao, Y.-L. Loo, Direct patterning of conductive water-soluble polyaniline for thin-film organic electronics. *Appl. Phys. Lett.* **86**, 074102 (2005).
36. L. F. Rozsnyai, M. S. Wrighton, Controlling the adhesion of conducting polymer films with patterned self-assembled monolayers. *Chem. Mater.* **8**, 309–311 (1996).
37. E. Smela, Thiol-modified pyrrole monomers: 4. Electrochemical deposition of polypyrrole over 1-(2-thioethyl)pyrrole. *Langmuir* **14**, 2996–3002 (1998).
38. C. D. Bain, E. B. Troughton, Y. T. Tao, J. Evall, G. M. Whitesides, R. G. Nuzzo, Formation of monolayer films by the spontaneous assembly of organic thiols from solution onto gold. *J. Am. Chem. Soc.* **111**, 321–335 (1989).
39. Z. Mekhalif, P. Lang, F. Garnier, Chemical pretreatment of platinum by aromatic and aliphatic thiols. Effect on polybithiophene electrodeposition and properties. *J. Electroanal. Chem.* **399**, 61–70 (1995).
40. C.-G. Wu, S.-C. Chiang, C.-H. Wu, Formation and electrochemical property of pyrrole-terminated SAMs and the effect of the SAMs on the physicochemical properties of polypyrrole films electrochemically deposited over them. *Langmuir* **18**, 7473–7481 (2002).
41. R. Cruz-Silva, M. E. Nicho, M. C. Reséndiz, V. Agarwal, F. F. Castillón, M. H. Farías, Electrochemical polymerization of an aniline-terminated self-assembled monolayer on indium tin oxide electrodes and its effect on polyaniline electrodeposition. *Thin Solid Films* **516**, 4793–4802 (2008).
42. S. Inaoka, D. M. Collard, Chemical and electrochemical polymerization of 3-alkylthiophenes on self-assembled monolayers of oligothiophene-substituted alkylsilanes. *Langmuir* **15**, 3752–3758 (1999).
43. R. A. Simon, A. J. Ricco, M. S. Wrighton, Synthesis and characterization of a new surface derivatizing reagent to promote the adhesion of polypyrrole films to N-type silicon photoanodes: N-(3-(trimethoxysilyl)propyl)pyrrole. *J. Am. Chem. Soc.* **104**, 2031–2034 (1982).
44. C.-G. Wu, H.-T. Hsiao, Y.-R. Yeh, Electroless surface polymerization of polyaniline films on aniline primed ITO electrodes: A simple method to fabricate good modified anodes for polymeric light emitting diodes. *J. Mater. Chem.* **11**, 2287–2292 (2001).
45. A. G. Sadekar, D. Mohite, S. Mulik, N. Chandrasekaran, C. Sotiriou-Leventis, N. Leventis, Robust PEDOT films by covalent bonding to substrates using in tandem sol–gel, surface initiated free-radical and redox polymerization. *J. Mater. Chem.* **22**, 100–108 (2012).
46. D. Bélanger, J. Pinson, Electrografting: A powerful method for surface modification. *Chem. Soc. Rev.* **40**, 3995–4048 (2011).
47. T. Nasir, L. Zhang, N. Vilà, G. Herzog, A. Walcarius, Electrografting of 3-aminopropyltriethoxysilane on a glassy carbon electrode for the improved adhesion of vertically oriented mesoporous silica thin films. *Langmuir* **32**, 4323–4332 (2016).
48. A. Adenier, M. M. Chehimi, I. Gallardo, J. Pinson, N. Vilà, Electrochemical oxidation of aliphatic amines and their attachment to carbon and metal surfaces. *Langmuir* **20**, 8243–8253 (2004).
49. V. Stockhausen, J. Ghilane, P. Martin, G. Trippé-Allard, H. Randriamahazaka, J.-C. Lacroix, Grafting oligothiophenes on surfaces by diazonium electroreduction: A step toward ultrathin junction with well-defined metal/oligomer interface. *J. Am. Chem. Soc.* **131**, 14920–14927 (2009).
50. J. Groppi, P. N. Bartlett, J. D. Kilburn, Toward the control of the creation of mixed monolayers on glassy carbon surfaces by amine oxidation. *Chemistry* **22**, 1030–1036 (2016).
51. D. E. Labaye, C. Jérôme, V. M. Geskin, P. Louette, R. Lazzaroni, L. Martinot, R. Jérôme, Full electrochemical synthesis of conducting polymer films chemically grafted to conducting surfaces. *Langmuir* **18**, 5222–5230 (2002).
52. A. Jacques, S. Devillers, J. Delhalle, Z. Mekhalif, Electrografting of in situ generated pyrrole derivative diazonium salt for the surface modification of nickel. *Electrochim. Acta* **109**, 781–789 (2013).
53. F. Ouhib, S. Desbief, R. Lazzaroni, S. Melinte, C. A. Duțu, C. Jerôme, C. Detrembleur, Electrografting onto ITO substrates of poly(thiophene)-based micelles decorated by acrylate groups. *Polym. Chem.* **4**, 4151–4161 (2013).
54. N. C. Tansil, H.-h. Yu, E. A. B. Kantchev, J. Y. Yang, Naphthalenetetracarboxylic diimide-grafted poly(3,4-ethylenedioxythiophene)s. *Polym. Prepr.* **48**, 74–75 (2007).
55. B. Barbier, J. Pinson, G. Desarmot, M. Sanchez, Electrochemical bonding of amines to carbon fiber surfaces toward improved carbon-epoxy composites. *J. Electrochem. Soc.* **137**, 1757–1764 (1990).
56. R. S. Deinhammer, M. Ho, J. W. Anderegg, M. D. Porter, Electrochemical oxidation of amine-containing compounds: A route to the surface modification of glassy carbon electrodes. *Langmuir* **10**, 1306–1313 (1994).
57. F. Geneste, C. Moinet, Electrochemically linking TEMPO to carbon via amine bridges. *New J. Chem.* **29**, 269–271 (2005).
58. R. Kumar, D. Leech, Immobilisation of alkylamine-functionalised osmium redox complex on glassy carbon using electrochemical oxidation. *Electrochim. Acta* **140**, 209–216 (2014).
59. O. Buriez, E. Labbé, P. Pigeon, G. Jaouen, C. Amatore, Electrochemical attachment of a conjugated amino–ferrocifen complex onto carbon and metal surfaces. *J. Electroanal. Chem.* **619–620**, 169–175 (2008).
60. S. Kesavan, S. B. Revin, S. A. John, Fabrication, characterization and application of a grafting based gold nanoparticles electrode for the selective determination of an important neurotransmitter. *J. Mater. Chem.* **22**, 17560–17567 (2012).
61. X. Crispin, R. Lazzaroni, V. Geskin, N. Baute, P. Dubois, R. Jérôme, J. L. Brédas, Controlling the electrografting of polymers onto transition metal surfaces through solvent vs monomer adsorption. *J. Am. Chem. Soc.* **121**, 176–187 (1999).

62. H. Sun, B.-y. Lu, D.-f. Hu, X.-m. Duan, J.-k. Xu, S.-j. Zhen, K.-x. Zhang, X.-f. Zhu, L.-q. Dong, D.-z. Mo, Electrosynthesis and characterization of aminomethyl functionalized PEDOT with electrochromic property. *Chin. J. Polym. Sci.* **33**, 1527–1537 (2015).
63. I. Gallardo, J. Pinson, N. Vilà, Spontaneous attachment of amines to carbon and metallic surfaces. *J. Phys. Chem. B* **110**, 19521–19529 (2006).
64. M. Tanaka, T. Sawaguchi, Y. Sato, K. Yoshioka, O. Niwa, Surface modification of GC and HOPG with diazonium, amine, azide, and olefin derivatives. *Langmuir* **27**, 170–178 (2011).
65. O. Buriez, F. I. Podvorica, A. Galtayriesc, E. Labbé, S. Top, A. Vessières, G. Jaouen, C. Combellas, C. Amatore, Surface grafting of a π-conjugated amino-ferrocifen drug. *J. Electroanal. Chem.* **699**, 21–27 (2013).
66. L. Bardini, M. Ceccato, M. Hinge, S. U. Pedersen, K. Daasbjerg, M. Marcaccio, F. Paolucci, Electrochemical polymerization of allylamine copolymers. *Langmuir* **29**, 3791–3796 (2013).
67. J. Ghilane, M. Delamar, M. Guilloux-Viry, C. Lagrost, C. Mangeney, P. Hapiot, Indirect reduction of aryldiazonium salts onto cathodically activated platinum surfaces: Formation of metal–organic structures. *Langmuir* **21**, 6422–6429 (2005).
68. S. Mahouche-Chergui, S. Gam-Derouich, C. Mangeney, M. M. Chehimi, Aryl diazonium salts: A new class of coupling agents for bonding polymers, biomacromolecules and nanoparticles to surfaces. *Chem. Soc. Rev.* **40**, 4143–4166 (2011).
69. P. A. Brooksby, A. J. Downard, Electrochemical and atomic force microscopy study of carbon surface modification via diazonium reduction in aqueous and acetonitrile solutions. *Langmuir* **20**, 5038–5045 (2004).
70. C. Saby, B. Ortiz, G. Y. Champagne, D. Bélanger, Electrochemical modification of glassy carbon electrode using aromatic diazonium salts. 1. Blocking effect of 4-nitrophenyl and 4-carboxyphenyl groups. *Langmuir* **13**, 6805–6813 (1997).
71. A. Adenier, C. Combellas, F. Kanoufi, J. Pinson, F. I. Podvorica, Formation of polyphenylene films on metal electrodes by electrochemical reduction of benzenediazonium salts. *Chem. Mater.* **18**, 2021–2029 (2006).
72. M. Herlem, B. Fahys, G. Herlem, B. Lakard, K. Reybier, A. Trokourey, T. Diaco, S. Zairi, N. Jaffrezic-Renault, Surface modification of p-Si by a polyethylenimine coating: Influence of the surface pre-treatment. Application to a potentiometric transducer as pH sensor. *Electrochim. Acta* **47**, 2597–2602 (2002).
73. E. W. H. Jager, O. Inganäs, I. Lundström, Microrobots for micrometer-size objects in aqueous media: Potential tools for single-cell manipulation. *Science* **288**, 2335–2338 (2000).
74. A. E. Daugaard, S. Hvilsted, T. S. Hansen, N. B. Larsen, Conductive polymer functionalization by click chemistry. *Macromolecules* **41**, 4321–4327 (2008).

Acknowledgments: We thank F. Deng for the assistance with FIB. **Funding:** This research was supported in part by the NIH through EUREKA grant 1RO1EB010892, by the Defense Advanced Research Projects Agency grant N66001-11-C-4190, by the National Science Foundation through grants DMR-1103027 and DMR-1505144, and by the University of Delaware. **Author contributions:** L.O. synthesized the monomers and performed electrochemical depositions and characterizations. B.W. performed FTIR measurements, ultrasonication tests, and FIB-SEM. All authors contributed to the initial draft. L.O. and D.C.M. wrote the final manuscript. D.C.M. conceived the project. **Competing interests:** D.C.M. is a cofounder and the chief scientific officer of Biotectix LLC, a University of Michigan spin-off company working to develop conjugated polymers to interface a variety of electronic biomedical devices with living tissue. All other authors declare that they have no competing interests. **Data and materials availability:** All data needed to evaluate the conclusions in the paper are present in the paper and/or the Supplementary Materials. Additional data related to this paper may be requested from L.O. and D.C.M.

Submitted 1 March 2016
Accepted 27 January 2017
Published 3 March 2017
10.1126/sciadv.1600448

Citation: L. Ouyang, B. Wei, C.-c. Kuo, S. Pathak, B. Farrell, D. C. Martin, Enhanced PEDOT adhesion on solid substrates with electrografted P(EDOT-NH_2). *Sci. Adv.* **3**, e1600448 (2017).